

Kinematic couplings for precision fixturing—Part I: Formulation of design parameters

A. H. Slocum*

A closed form analysis for the design of a three-groove kinematic coupling is developed and used to design a 356 mm (14 in) diameter kinematic coupling with 28.6 mm (1-1/8 in) diameter balls and 45 kN (10000 lbf) preload. When the coupling is subjected to cutting loads in the order of 75 N (17 lbf), the resulting wall thickness errors in a 254 mm (10 in) diameter hemispherical part are: (1) a 0.36 μm (14 μin) error from the cutting force, and (2) a 0.89 μm (35 μin) error with a 2% preload error. If ceramic balls and grooves are used, fretting corrosion of the coupling interface can be avoided and the coupling can operate in a corrosive environment. The kinematic design is unaffected by film contamination and does not require an extensive wear-in period. Preliminary experiments show the coupling to be repeatable to $\pm 0.25 \mu\text{m}$ ($\pm 10 \mu\text{in}$).

Keywords: kinematic couplings, fixture mounting, closed form analysis, robotics, engineering design

Introduction

Two schools of thought exist as to the best way to locate two surfaces with respect to each other: kinematic design; and design for elastic averaging. As discussed by Evans¹ in his assessment of the history of precision engineering, 'Contrast, for example Pollard², in the introduction to his monograph on instrument design, bewailing non-kinematic design practices he attributes to machine tool design practice being brought to instrument design and Rosenhain³ who bewails the flimsy designs of instrument makers and calls for an approach more akin to machine tool design'.

This paper addresses formulation of design parameters and characteristics of a precision coupling for mounting fixtures (eg pot chucks) to precision spindles. For the intended application, the coupling has to locate a 254 mm (10 in) diameter vacuum chuck with respect to the faceplate of a lathe with a maximum allowable resulting wall thickness error in the order of 1.3 μm (50 μin). Cutting loads are assumed to be in the order of 45 N (10 lbf) from each of three orthogonal directions.

Coupling requirements

To position and orientate a fixture (eg vacuum chuck) with respect to the faceplate of a lathe, six degrees of freedom must be established. If the coupling is not overconstrained (ie has only six

contact points) its structure can be considered deterministic, and the motion of the system can be represented by a closed form solution. However, with only six contact points, stiffness might be low, and brinelling of the interfaces may occur. If more than six contact points exist, then the system can be stiffer but will also be overconstrained, which prevents modelling the structure in closed form and increases design engineering costs. This also increases the chance of manufacturing errors and of contamination from the machining environment degrading repeatability. Thus an ideal coupling might have the following characteristics:

- stiffness of the coupling in the order of the stiffness of machine and part being coupled;
- accuracy unaffected by particle or film contamination of the coupling interface;
- repeatability on the sub-micron level;
- robotically changeable.

Kinematic couplings

A kinematic coupling is not overconstrained and is not very sensitive to contamination, on account of its discrete number of contact points. Repeatability of kinematic couplings can be in the order of microinches.** Two types of kinematic couplings are most frequently used. The first is a ball-flat-groove coupling shown in Fig 1 (a). It has a ball resting on or in each of these geometries. Because the coupling is not symmetric, it is not suited for use in high speed turning operations. The

* Center for Systems Automation, Massachusetts Institute of Technology, 77 Massachusetts Avenue, Room 1-143, Cambridge, MA 02139, USA and Automated Production Technology Division, National Bureau of Standards, Gaithersburg, MD 20899, USA

** Discussions with Dr Robert J. Hocken, Chief Precision Engineering Division, National Bureau of Standards, Gaithersburg, MD, USA

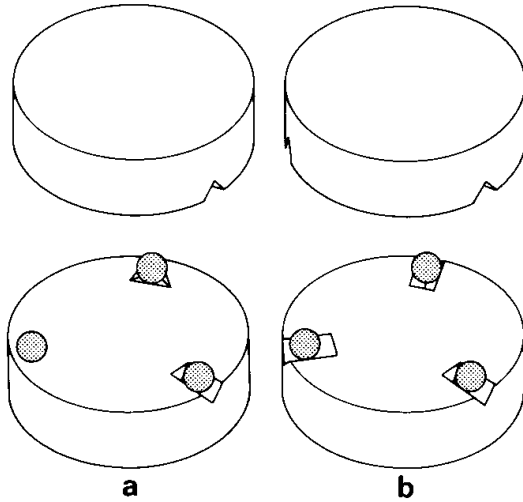


Fig 1 (a) Flat-groove-trihedron kinematic coupling; (b) three-groove kinematic coupling

second type is shown in Fig 1 (b) and consists of three radial grooves in each of two plates with three balls in the grooves. The normals to the six contact surfaces are not parallel, thus the relative position and orientation of the two plates coupled by the balls is uniquely defined. Successful design of the coupling depends on controlling parameters at the contact points: keeping contact stresses well below the yield point of the material; maintaining high stiffness; and preventing fretting corrosion.

In addition, the location of the plane of coupling action affects performance. For a hemispherical part of radius R_h , the effect of angular orientation errors in the coupling will cause Abbe errors in the location of the centre of the fixture. The effect of translational errors ΔX , ΔY and ΔZ in the location of the fixture's centre will cause an error in wall thickness Δt at any point θ , ϕ on the hemispherical shell of:

$$\Delta t = \Delta X \cos \theta \cos \phi + \Delta Y \sin \theta \cos \phi + \Delta Z \sin \phi \quad (1)$$

Thus the plane of coupling should be located near the part equator.

Elastic characteristics of the ball-groove interface

For simple curved surfaces in contact, the application of plane Hertz theory is based on the gap bending hypothesis which states that the effect of geometry on the system in the contact region is a function of the algebraic sum of the curvatures of the two surfaces. Thus, contact between two curved surfaces can be reduced to contact between a plane and an equivalent surface. Errors in this assumption are on the order of 10%⁴.

The geometry of the coupling is defined by the major and minor radii of the ball (R_b) and groove ($(R_b[1 + \eta])$ and ∞), respectively. The radius of an equivalent ball on a flat plate is R_e and is the inverse of the sum of the curvatures of the ball and

groove:

$$R_e = \frac{R_b(1 + \eta)}{(1 + 2\eta)} \quad (2)$$

With a contact force F and an equivalent Young's modulus for the two bodies $1/E^*$ $= (1 - \nu_1^2)/E_1 + (1 - \nu_2^2)/E_2$, the footprint of the contact region will be approximately circular with a radius of a :

$$a = \left(\frac{3FR_e}{2E^*} \right)^{1/3} \quad (3)$$

For the ball seated between two grooves, the distance of approach of two far field points in the grooved structure will be:

$$\delta = 2 \left(\frac{1 + 2\eta}{R_b(1 + \eta)} \right)^{1/3} \left(\frac{3F}{2E^*} \right)^{2/3} \quad (4)$$

The maximum contact pressure will be σ_0 :

$$\sigma_0 = \frac{1}{\pi} \left(\frac{1 + 2\eta}{R_b(1 + \eta)} \right)^{2/3} \left(\frac{3(E^*)^2 F}{2} \right)^{1/3} \quad (5)$$

The effect of the ball-groove radius ratio η on the contact stress is shown in Fig 2. To avoid problems with contamination at the interface, η should be as large as possible. To minimize the effect on contact stress and deflection, η should be as small as possible. If the effect on stress caused by increasing η is kept at a 10% level, which is in the order of the error in the Hertz calculations, then a good compromise is to let $\eta = 0.20$.

The ratio of the preload to the applied load also has a large effect on the stiffness of the system. If the cutting force F_c is represented as a percentage ζ of the preload F_p , then the deflection varies as:

$$\delta \propto F_p^{2/3} \{ (1 + \zeta)^{2/3} - 1 \} \quad (6)$$

Fig 3 shows an effectively linear relation for this function over a range of expected values for ζ . As expected, the ratio of applied load to preload should be kept as small as possible.

If the coupling's geometry is designed to have a specific deflection at a set preload and applied load (applied load initially specified as $F_c = \zeta F_p$),

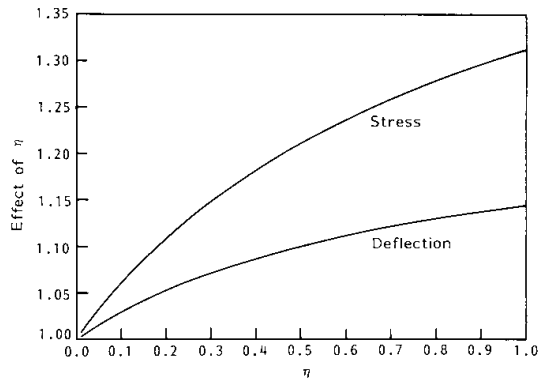


Fig 2 $R_g = R_b(1 + \eta)$; effect of ball-groove radius ratio η on stress and deflection

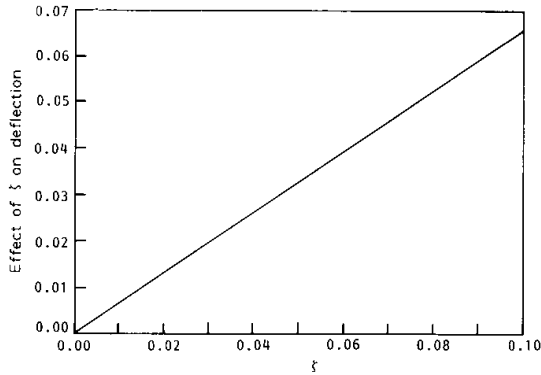


Fig 3 $F_c = \zeta F_p$; effect of ζ , ratio of applied force to preload, on deflection

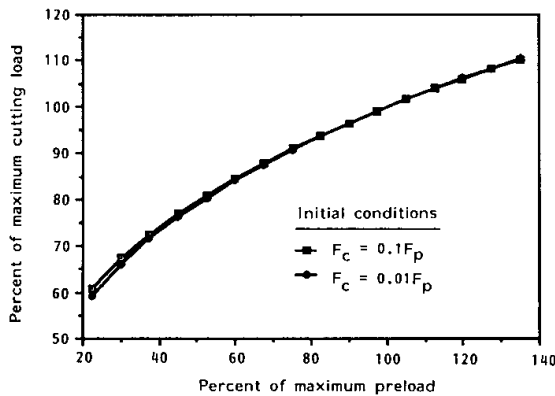


Fig 4 Change in preload, as a function of cutting load, required to maintain constant deflection

what percentage decrease α in applied load must accompany a change in preload in order to maintain a constant deflection? From Eqs (4) and (6) with the preload given by $F_{p\text{-new}} = \lambda F_{p\text{-old}}$ and the cutting force given by $F_{c\text{-new}} = \alpha F_{c\text{-old}}$,

$$\alpha_c = \left\{ \frac{(1 + \zeta)^{2/3} - 1}{\lambda^{2/3} + 1} \right\}^{3/2} - 1 \quad (7)$$

Fig 4 shows the relation between a percentage change in preload and the corresponding change in allowable cutting force required to maintain a constant deflection. Values for ζ of 0.1 and 0.01 were used, and they have very little effect on the value of α . For values of η that are considered and their effect on allowable preload ($\eta < 0.2$), changes in preload are in the order of 30%; thus the region of interest centred about 100% in Fig 4 is linear. Hence, the rule of thumb: a percentage change X in the allowable preload must be accompanied by a percentage change $X/2$ in the applied cutting force if the deflection is to remain constant.

Static analysis of a three-groove kinematic coupling

In this section are formulated the governing static

and kinematic equations for a three-groove kinematic coupling to be used for holding hemispherical vacuum chucks to the faceplate of a precision lathe.

The loading diagram for the three-groove coupling is shown in Fig 5. Assuming that contact between surfaces is frictionless, the force moment balance equations for this system can be expressed in the following matrix form*:

$$\begin{bmatrix} 1/2 & 0 & -1 & 0 & 1/2 & 0 \\ \sqrt{3}/2 & 0 & 0 & 0 & -\sqrt{3}/2 & 0 \\ 0 & 1 & 0 & 1 & 0 & 1 \\ 0 & -R/2 & 0 & R & 0 & -R/2 \\ 0 & -R\sqrt{3}/2 & 0 & 0 & 0 & R\sqrt{3}/2 \\ R & 0 & R & 0 & R & 0 \end{bmatrix}$$

$$\begin{bmatrix} F_{1N} \\ F_{1Z} \\ F_{2N} \\ F_{2Z} \\ F_{3N} \\ F_{3Z} \end{bmatrix} = \begin{bmatrix} C_1 \\ C_2 \\ C_3 \\ C_4 \\ C_5 \\ C_6 \end{bmatrix} = \begin{bmatrix} F_{CX} \\ -F_{CY} \\ -3F_{PZ} - F_{CZ} \\ -R_C F_{CZ} \sin \theta + I F_{CY} \\ R_C F_{CZ} \cos \theta - I F_{CX} \\ R_C F_{CX} \sin \theta - R F_{CY} \cos \theta \end{bmatrix} \quad (8)$$

Solving Eq (8) yields:

$$F_{1N} = \frac{\sqrt{3}C_1 R + 3C_2 R + \sqrt{3}C_6}{3\sqrt{3}R} \quad (9)$$

$$F_{2N} = \frac{-2C_1 R + C_6}{3R} \quad (10)$$

$$F_{3N} = \frac{\sqrt{3}C_1 R - 3C_2 R + \sqrt{3}C_6}{3\sqrt{3}R} \quad (11)$$

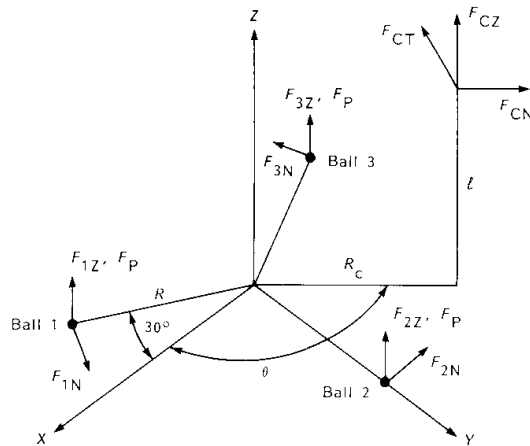


Fig 5 Loadings and reaction forces on three-groove kinematic coupling

* Note that $F_{CX} = F_{CN} \cos \theta - F_{CT} \sin \theta$, and $F_{CY} = F_{CN} \sin \theta + F_{CT} \cos \theta$

$$F_{1z} = \frac{C_3 R - C_4 - \sqrt{3} C_5}{3R} \quad (12)$$

$$F_{2z} = \frac{C_3 R + 2C_4}{3R} \quad (13)$$

$$F_{3z} = \frac{C_3 R - C_4 + \sqrt{3} C_5}{3R} \quad (14)$$

As discussed above, for maximum stiffness the ball-groove interface should be designed as shown in Fig 6. The resultant forces on any ball 'i' are decomposed into the groove normal forces F_{GLi} and F_{GRi} that are applied directly to the balls. The Z direction force is always pushing the ball into the groove, thus the adoption of a sign convention 'positive' for Z direction forces into the groove:

$$F_{GLi} = \frac{F_{Gzi} - F_{Gni}}{\sqrt{2}} \quad (15)$$

$$F_{GRi} = \frac{F_{Gzi} + F_{Gni}}{\sqrt{2}} \quad (16)$$

Since the forces applied to the ball are orthogonal, superposition of the deflections δ_{GLi} and δ_{GRi} is assumed to be valid. The resulting motions of the point on the coupling just above the ball with respect to its initial location are:

$$\delta_{zi} = -(\delta_{GLi} + \delta_{GRi})/\sqrt{2} \quad (17)$$

$$\delta_{ni} = (-\delta_{GLi} + \delta_{GRi})/\sqrt{2} \quad (18)$$

The motion at the centre of the hemishell is of primary concern. Assuming that the plane of the coupling is located at the equator of the part, for ball 1 the effect of the deflection δ_{z1} on the motion of the centre of the hemishell is:

$$\delta_{cz1x} = -\frac{\delta_{z1}^2}{3\sqrt{3}R} \quad (19)$$

$$\delta_{cz1y} = \frac{\delta_{z1}^2}{9R} \quad (20)$$

$$\delta_{cz1z} = \frac{\delta_{z1}}{3} \quad (21)$$

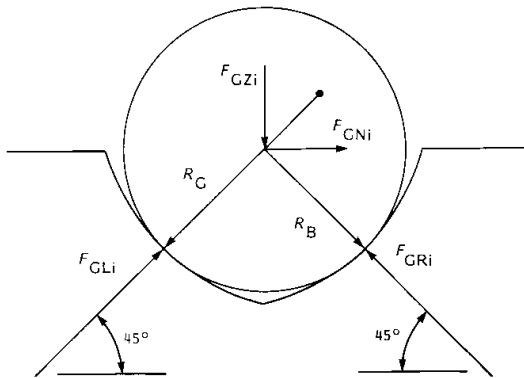


Fig 6 Forces on the ball and gothic arch of a three-groove kinematic coupling

Motions at the centre of the hemishell caused by balls 2 and 3 are mapped from the above with coordinate rotations of 120° and 240°, respectively.

The motion normal to the grooves in the XY plane also induces motion at the centre of the hemishell. With the assumption of rigid body motion, when ball 1 moves in a direction normal to its groove in the XY plane an amount δ_{N1} , the new coordinates of ball 1 are:

$$X_{11} = R\sqrt{3}/2 + 0.5\delta_{N1} \quad (22)$$

$$Y_{11} = -0.5R + \delta_{N1}\sqrt{3}/2 \quad (23)$$

The X coordinate of ball 2 is geometrically fixed by the groove which is parallel to the Y axis. The new Y coordinate of ball 2 caused by δ_{N1} motion of ball 1 is found assuming the distance between the balls must remain constant:

$$Y_{21} = Y_{11} + 2(3R^2 - X_{11}^2)^{1/2} \quad (24)$$

The new coordinates of ball 3 are found in a similar manner, with the constraint that the X and Y coordinates are related by the orientation of the groove:

$$X_{31} = Y_{31}\sqrt{3}/2 \quad (25)$$

$$Y_{31} = \frac{\sqrt{3}X_{11} + Y_{11} - [12R^2 - (X_{11} - Y_{11}\sqrt{3})^2]^{1/2}}{4} \quad (26)$$

The centre of the hemishell is at the centroid of the equilateral triangle formed by the three balls. The X and Y motions of the centre of the hemishell caused by the groove normal deflection of ball 1 is thus:

$$\delta_{CN1X} = (X_{11} + X_{21} + Y_{31})/3 \quad (27)$$

$$\delta_{CN1Y} = (Y_{11} + Y_{21} + Y_{31})/3 \quad (28)$$

The effects of the groove normal deflections of the other balls on the motion of the centre of the hemishell are found on the basis of the symmetry of the design.

Once the motion of the centre of the hemishell part that is being held in the vacuum chuck has been found, the effect on the part's wall thickness can be determined by Eq (1).

Effects of dynamic forces

If a 90 kg (200 lb) part is mounted 0.13 mm (0.005 in) off centre, then at 300 rev/min a static imbalance force of about 12 N will be created. This may not be significant in terms of its effect on the coupling if stiffness is in the order of $1.7 \times 10^8 \text{ N m}^{-1}$, but it warrants further investigation into the static and dynamic balance properties of the total system. In particular, the latter may be much larger if the part is placed in the vacuum chuck and the equator of the part is not exactly parallel to the equator of the vacuum chuck.

Design example

Two materials are considered for this application—hardened steel and a ceramic (eg silicon carbide or silicon nitride). Figs 3, 4 and 5 provided a guiding

methodology for initial sizing of system components. For this analysis, the groove radius was chosen to be 1.2 times the ball radius ($\eta = 0.2$). The maximum outside radius (to the outside edges of the balls) of the coupling was fixed by the application to be 178 mm (7.0 in), and the cutting force acted at a radius of 127 mm (5.0 in). The position of the cutting force along the hemishell was found to affect the results only by about 10%, and was thus kept applied at the worst case location, near the pole. Figs 7 and 8 show the ball radius as a function of contact stress and applied preload. These curves are to be used in conjunction with the load/deflection curves for the coupling, so a reasonable ball size and preload can be chosen for the design.

The first step is to determine the optimal location of the plane of coupling action. Fig 9 shows the effect of the Abbe error produced as the plane of coupling action is moved away from the plane of the hemishell's equator. The loading in this case consists of 45 N cutting force in each of the X, Y and Z directions, and a 1113 N force due to the weight of the part and the pot chuck. Beyond 50 mm (2 in), the error becomes very large; thus the plane of coupling action should be located as close as possible to the hemishell's equator. For all

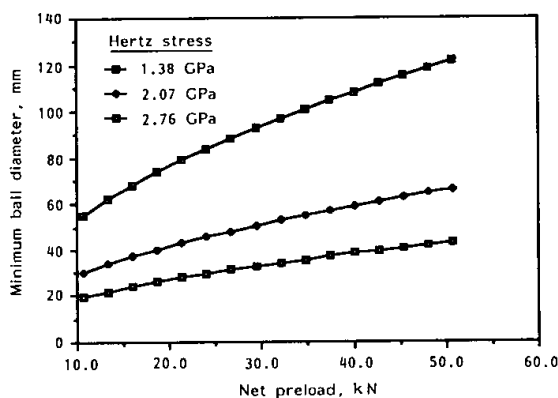


Fig 7 Required ball radius for steel balls

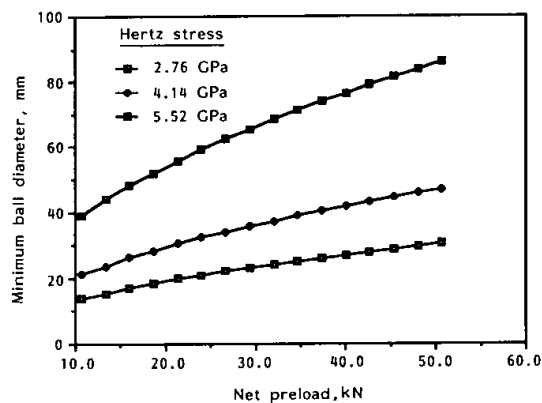


Fig 8 Required ball radius for silicon carbide balls

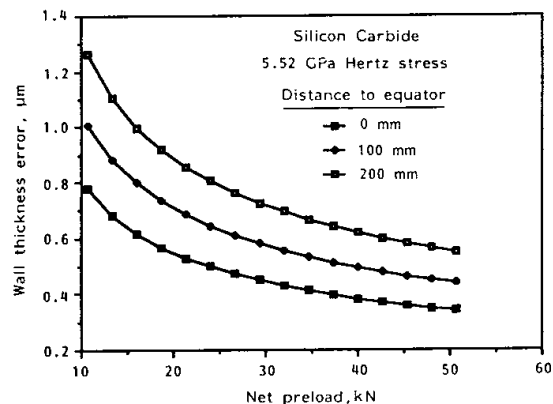


Fig 9 Abbe error caused by moving plane of coupling action away from hemishell's equator

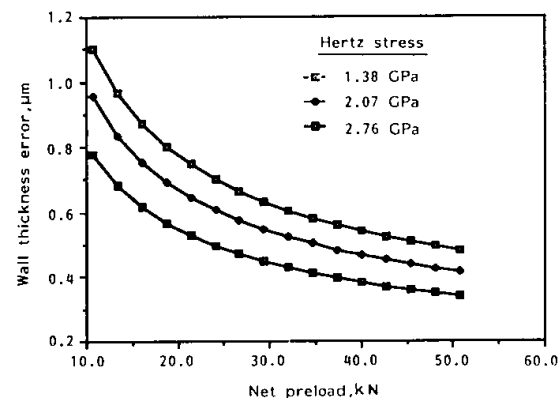


Fig 10 Performance of steel three-groove kinematic coupling

subsequent analysis it is assumed that the two are coincident.

The next step is to determine the wall thickness errors as a function of preload and contact stress. For the intended application on a lathe, gravity-induced deflections will be in a non-sensitive direction and are not considered. Figs 10 and 11 show the performance of the steel and silicon carbide couplings, respectively.

For the steel coupling to be viable, a maximum contact stress of 2.8 GPa is needed to keep the ball diameter at a reasonable value of about 28.6 mm with a preload of 22 kN. Lowering the preload results in deflections much greater than the ceramic coupling. With these parameters, the best performance obtainable from the steel coupling is a wall thickness error of about 0.74 μm (29 μin).

For the silicon carbide coupling, the preload can be increased to 45 kN while maintaining a ball diameter of 28.6 mm if the allowable stress is increased to 5.5 GPa. The maximum allowable contact stress for silicon carbide is in the order of 6.9 GPa. Under these conditions, the error in wall thickness is in the order of 0.36 μm (14 μin). If the contact stress is lowered to 4.2 GPa, in the interest of safeguarding against fracture of the ceramic, then

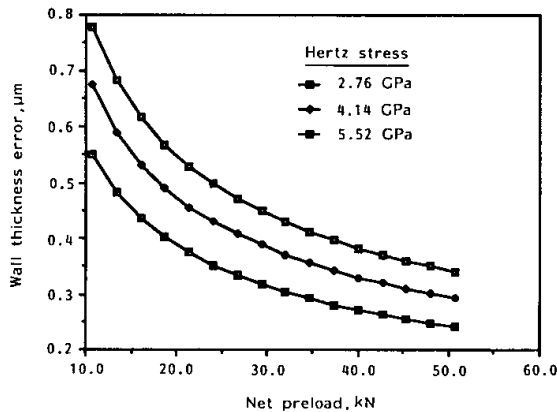


Fig 11 Performance of silicon carbide three-groove kinematic coupling

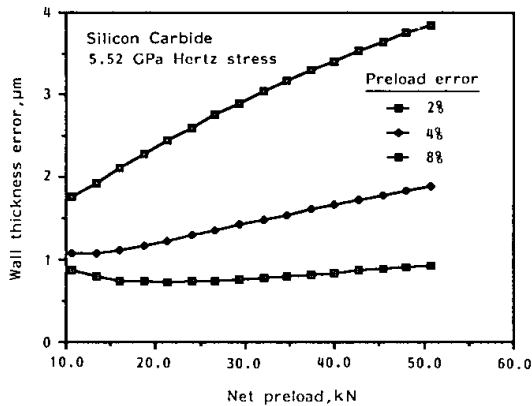


Fig 12 Effect of repeatability of preload on coupling performance

the best performance for 28.6 mm balls results in an error in the order of about 0.48 µm (19 µin).

The preload must be applied in a very repeatable manner or errors will result. Because the contour of the hemispherical chuck is to be machined *in situ*, if the preload on the coupling varies with use then the coupling will deform differently, and errors will result. An analysis of these changing preload effects on the pot chuck itself is beyond the scope of this paper and is the subject of future work. With respect to the kinematic coupling, an error in the preload will change the Z position only. This could be compensated for with a tool offset. Fig 12 shows the effect of 2, 4 and 8% errors in preload on wall thickness errors. By keeping preload errors below the 2% level, for preloads up to 45 kN the errors will be in the order of 0.89 µm (35 µin). A solid model representation of the design is shown in Fig 13.

Effects of contamination on the coupling interfaces

Minimizing contamination of the coupling interface may require cleaning with a solvent such as freon.

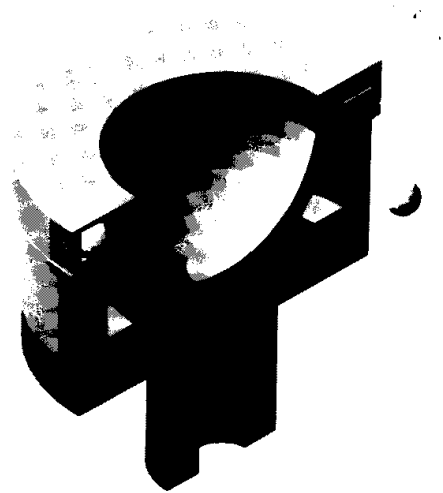


Fig 13 Solid-model representation of a kinematic coupling used to hold a pot chuck

However, removing all the dirt and oil can lead to fretting corrosion of metal surfaces.

Fretting corrosion is caused by repeated alternating sliding contact of two adjacent surfaces. As noted by O'Connor⁵, damage can occur with slip amplitude as small as 1 µm (40 µin), and Tomlinson⁶ puts the figure at values as low as 0.03 mm (1 µin). This value is also indicated by Waterhouse⁷. The action of fretting tends to increase the coefficient of friction until stresses high enough to initiate a fatigue crack form. For the kinematic coupling with its high contact stresses, this could be a problem. Also, metal to metal contact results in higher coefficients of friction. This occurs when metal to metal contact causes local cold welds between asperities which are then torn apart. The newly exposed fresh metal surface quickly oxidizes and the process repeats.

Fretting can be prevented by using ceramics for the balls and grooves. A ceramic such as silicon carbide has a Hertz strength in the order of 6.9 GPa, a Young's modulus of 415 GPa, and a fatigue life approximately one to two orders of magnitude higher than for bearing steels⁸. However, fracture toughness of silicon carbide is about one-third that of SAE 52100 bearing steel, so care during handling is required. Another alternative is silicon nitride which has a Hertz strength on the order of 6.9 GPa (and a Young's modulus of 311 GPa). Silicon nitride has been made tough enough to allow it to be certified for gas turbine engine ball bearings. For a silicon nitride kinematic coupling, the silicon carbide wall thickness errors can be scaled by $(415/311)^{2/3} = 1.20$.

Manufacturing considerations for kinematic couplings

The above design considered the use of silicon carbide balls which are currently not commercially

available. Grade 5 silicon nitride balls are available with a diameter of 28.6 mm (1-1/8 in) and surface finish on the order of $0.01 \mu\text{m}$ ($0.5 \mu\text{in}$). Custom manufactured gothic arch shapes are also available with similar surface finishes. It is even possible to manufacture the entire structure from silicon nitride (or silicon carbide) using powder metallurgy techniques. Because the coupling is self-aligning, if the final shape of the chuck is finished using the machine on which the chuck is to be mounted, then tolerances on the parts need not be greater than approximately 0.13 mm (0.005 in). The assembly may, however, need to be dynamically balanced.

To minimize the chance of one chuck held by the coupling influencing a different chuck, the balls should be mounted in the chucks. Each set of balls (for each chuck) should be set at a slightly different radius; thus each chuck's balls will have their own unique contact regions in the gothic arches and they will be unaffected by the use of other chucks.

Conclusions

This paper has addressed some of the issues involved in designing high accuracy fixturing systems for turning centres. A three-groove kinematic coupling was found to have the following characteristics.

- (1) With 28.6 mm (1-1/8 in) diameter silicon carbide balls, 17.15 mm (0.675 in) radius gothic arches, 45 kN preload and cutting forces of $F_x = F_y = F_z = 45 \text{ N}$, a 356 mm (14 in) diameter coupling produces the following wall thickness errors in a 254 mm (10 in) diameter hemispherical part:
 - (a) $0.36 \mu\text{m}$ ($14 \mu\text{in}$) error from cutting force;
 - (b) $0.89 \mu\text{m}$ ($35 \mu\text{in}$) error with 2% additional preload error.
- (2) Because the coupling has only six discrete contact points, the system is not sensitive to fluid contamination and less sensitive to dirt than traditional curvic or Hirth couplings.
- (3) The proposed use of silicon carbide or silicon nitride balls and grooves would make the system immune to chemical attack.
- (4) By mounting the balls for each chuck at slightly different radii than for other chucks, a crash with one chuck should not affect the accuracy of other chucks.
- (5) The high surface finish of $0.01 \mu\text{m}$ ($0.5 \mu\text{in}$) attainable with ceramics will enable the couplings to be used without requiring a wear-in period.

The analysis assumed that the behaviour at the coupling interface was frictionless and could be modelled by Hertz contact theory. If steel were used for the coupling, friction would be present, and the danger of fretting would exist. If silicon nitride or silicon carbide were used, the coefficient of friction would be very low (μ in the order of 0.01) and the validity of the assumptions made would be increased.

A solid-model representation of the design is shown in Fig 13. Preliminary tests of a 356 mm (14 in) coupling made with steel arches (chosen for economy) and silicon nitride balls indicate repeatability of $\pm 0.25 \mu\text{m}$ ($10 \mu\text{in}$) with no wear-in period required. Detailed results of these tests will be presented in a subsequent paper*.

Acknowledgements

This work was sponsored by Martin Marietta Energy Systems Inc for the US Department of Energy under Contract No DE-AC05-84OR21400. The author also wishes to thank Norton Advanced Ceramics Co for their technical assistance.

References

- 1 Evans C. *Precision engineering: an evolutionary perspective*, MSc Thesis, Cranfield Inst. of Technol., Cranfield, UK, March 1987
- 2 Pollard *The kinematical design of couplings in instruments*, Adam Hilger Publ., Bristol, UK, 1929
- 3 Rosenhain W. The mechanical design of instruments. In *Proc. the Optical Convention, London, 1905*
- 4 Tripp J. H. *Hertzian contact in two and three dimensions*, NASA Technical Paper 2473, July 1985
- 5 O'Connor J. J. The role of elastic stress analysis in the interpretation of fretting fatigue failures. In *Fretting fatigue*, Waterhouse (ed), Applied Science Publishers, London, 1981, p 23
- 6 Tomlinson G. A. et al *Proc. Inst. Mech. Engrs.*, 1939, 141, p 223
- 7 Waterhouse, R. B. Avoidance of fretting failures. In *Fretting fatigue*, Waterhouse (ed), Applied Science Publishers, London, 1981, p 238
- 8 Walker, J. R. Properties and applications for silicon nitride in bearings and other related components. Paper presented at the *Workshop on Conservation and Substitution Technology for Critical Metals in Bearings and Related Components for Industrial Equipment and Opportunities for Improved Performance*, Vanderbilt Univ., Nashville, TN, 12-14 March 1984

*Kinematic couplings for precision fixturing—Part II: Experimental determination of repeatability and stiffness

